

## Differences in nucleotide compartmentation and energy state in isolated and in situ rat heart: assessment by $^{31}\text{P}$ -NMR spectroscopy

John P. Williams, John P. Headrick \*

*From the Department of Physiology and Pharmacology School of Molecular Sciences, James Cook University of North Queensland, Townsville, Queensland 4811, Australia*

Received 26 February 1996; accepted 11 April 1996

### Abstract

Free cytosolic concentrations of ATP, PCr, ADP and 5'-AMP, and the cytosolic  $[\text{ATP}]/[\text{ADP}][\text{P}_i]$  ratio, were determined in isolated and in situ rat hearts using  $^{31}\text{P}$ -NMR spectroscopy. Total tissue metabolite concentrations were determined by HPLC analysis of freeze-clamped, perchloric acid-extracted tissue. In in situ myocardium the PCr/ATP ratio was  $2.7 \pm 0.2$  determined from  $^{31}\text{P}$ -NMR data (using either PCr/ $\beta$ -NTP or PCr/ $\gamma$ -NTP), and  $1.9 \pm 0.1$  ( $P < 0.01$ ) determined from total tissue concentrations.  $^{31}\text{P}$ -NMR-determined and total tissue [PCr] were in excellent agreement ( $49.6 \pm 8.4$  and  $49.5 \pm 1.0 \mu\text{mol.g}^{-1}$  dry wt, respectively), whereas  $^{31}\text{P}$ -NMR-determined [ATP] ( $18.6 \pm 3.2 \mu\text{mol.g}^{-1}$  dry wt) was only 71% of the total tissue concentration ( $26.1 \pm 1.7 \mu\text{mol.g}^{-1}$  dry wt,  $P < 0.01$ ). Isolation and Langendorff perfusion of rat hearts with glucose as substrate reduced total tissue [ATP] and [PCr] and the  $^{31}\text{P}$ -NMR-determined PCr/ATP ratio fell to  $1.5 \pm 0.1$ . This value agreed well with the total tissue ratio of  $1.4 \pm 0.1$ , and there was excellent agreement between  $^{31}\text{P}$ -NMR-determined and total tissue [PCr] and [ATP] values in the perfused heart. Addition of pyruvate to perfusate increased the  $^{31}\text{P}$ -NMR-determined PCr/ATP ratio to  $1.7 \pm 0.1$  due to elevated [PCr], and there remained excellent agreement between NMR-determined and total tissue [PCr] and [ATP] values. Free cytosolic [ADP] (from the creatine kinase equilibrium) was 5% of total tissue ADP, and free cytosolic [5'-AMP] (from the adenylate kinase equilibrium) ranged from 0.2–0.3% of total tissue 5'-AMP. Bioenergetic state, indexed by  $[\text{ATP}]/[\text{ADP}][\text{P}_i]$ , was much lower in isolated perfused hearts ( $30 \text{ mM}^{-1}$ ) vs. in situ myocardium ( $\sim 150 \text{ mM}^{-1}$ ). In summary, we observe a substantial disproportionality between total tissue PCr/ATP and  $^{31}\text{P}$ -NMR-determined PCr/ATP in highly energised in situ myocardium but not in isolated perfused hearts. This appears due to an NMR invisible ATP compartment approximating 29% of total tissue ATP in situ. Additionally, more than 95% of ADP and more than 99% of 5'-AMP exist in bound forms in perfused and in situ myocardium. The physiological significance of these observations is unclear. However, substantial differences between  $^{31}\text{P}$ -NMR visible and total tissue [ATP] introduces significant errors in conventional estimation of free cytosolic [ADP], [5'-AMP] and  $[\text{ATP}]/[\text{ADP}][\text{P}_i]$  from in vivo  $^{31}\text{P}$ -NMR data.

**Keywords:** Adenosine triphosphate; Creatine phosphate; NMR visibility; Cytosolic concentration; Rat heart; Phosphorylation ratio

### 1. Introduction

The question of compartmentation of myocardial adenine nucleotides has challenged scientists for a number of years. Conventional analyses reveal distinct compartmentation of 5'-AMP between cytosolic and mitochondrial fractions [1,2]. Substantial differences between total and free cytosolic ADP may be primarily due to actomyosin binding [1,2]. Results for ATP are more controversial, although evidence supports between 7–30% localisation of myocardial ATP in mitochondria [1–6].

$^{31}\text{P}$ -NMR spectroscopy not only offers a powerful tool for non-invasive investigations of cellular metabolism [7,8], but also provides us with an alternate method of examining intracellular compartmentation of phosphate metabolites [9–11]. For example, we recently employed NMR to study compartmentation of phosphate and the kinetics of changes in free and bound phosphate in ischaemic rat heart [12]. However, from a methodological viewpoint compartmentation and partial NMR visibility of nucleotides may introduce errors in  $^{31}\text{P}$ -NMR analysis of cellular metabolism and energy state. Metabolite compartmentation represents both a research challenge and a potential source of error for  $^{31}\text{P}$ -NMR studies.

$^{31}\text{P}$ -NMR investigations of myocardial nucleotide visibility are restricted to isolated perfused hearts, and con-

\* Corresponding author. Fax: +61 77 251394; e-mail: john.headrick@jcu.edu.au

flicting results have been obtained in this model. Humphrey and Garlick [10] and Bak and Ingwall [11] observe excellent agreement between total tissue and  $^{31}\text{P}$ -NMR visible ATP under basal conditions in perfused rat hearts. Alternatively, Takami et al. calculate ATP to be only 60% NMR visible [9]. During ischaemia Takami et al. [9] and Humphrey and Garlick [10] document reductions in ATP visibility, whereas other groups obtain no evidence of changes in the NMR visibility of ATP during ischemia or hypoxia [11–15]. Similar controversy exists for liver where some studies suggest that ATP is less than 100% NMR visible [16], while others indicate that NMR-determined and total tissue ATP values are comparable [17]. To date no studies have examined NMR visibility or apparent compartmentation of high-energy phosphates in the myocardium *in situ*, and few studies have addressed the energy state of *in situ* myocardium relative to the isolated perfused heart. Here, we address the question of high-energy phosphate visibility or compartmentation in the *in situ* and perfused rat myocardium.  $^{31}\text{P}$ -NMR-determined ATP and PCr concentrations (assumed to reflect freely mobile cytosolic levels), and free cytosolic [ADP] and [5'-AMP] calculated from enzyme equilibria, are compared with HPLC-determined concentrations of these compounds (assumed to reflect total tissue levels). The data allows an assessment of the fundamental question of metabolite compartmentation in the myocardium, and of the validity of current calibration strategies employed in *in vivo*  $^{31}\text{P}$ -NMR studies.

## 2. Materials and methods

### 2.1. Isolated perfused heart preparation

The isovolumic Langendorff perfused rat heart preparation used to simultaneously acquire  $^{31}\text{P}$ -NMR spectral and functional data has been described in detail previously [18–20]. Male Sprague-Dawley rats were anaesthetised with 50 mg.kg $^{-1}$  sodium pentobarbitone administered intraperitoneally. A thoracotomy was performed and hearts rapidly excised into ice-cold perfusion fluid. The aorta was cannulated and hearts perfused via the aorta at a constant pressure of 100 mmHg. Perfusion fluid was a modified phosphate-free Krebs-Henseleit buffer containing (in mM): NaCl 120, NaHCO $_3$  25, KCl 4.7, CaCl $_2$  1.25, MgCl $_2$  1.2, glucose 15, and EDTA 0.05. In a second groups of hearts substrate was changed to 5 mM glucose + 10 mM pyruvate. Buffer was equilibrated with 95% O $_2$ , 5% CO $_2$  and maintained at 37°C, giving a pH of 7.4. The left ventricle was vented through the apex and a fluid filled latex balloon introduced into the ventricle via the mitral valve. The balloon was attached by a fluid filled line to a Statham P23XL pressure transducer, and was filled using a 500- $\mu\text{l}$  glass syringe. For quantitation of  $^{31}\text{P}$  spectral intensities the ventricular balloon was filled with a 35 mM methylene

diphosphonate (MDP) solution in 120 mM KCl. The MDP concentration was verified by atomic absorption spectrophotometry.

$^{31}\text{P}$ -NMR spectra were acquired at 121.46 MHz from isolated hearts in a 7 Tesla superconducting magnet, as described in detail previously [18,19]. Hearts were enclosed in a fluid-filled chamber and were situated within the sensitive volume of a double-tuned  $^1\text{H}/^{31}\text{P}$  NMR coil. The magnet was initially shimmed on the heart/perfusate  $^1\text{H}$  signal.  $^{31}\text{P}$  acquisitions employed a 10 kHz sweep width and consisted of 4096 data points. After a 30-min stabilisation period, 3 consecutive fully relaxed spectra were acquired. The spectra consisted of 60 signal averaged FID's acquired with an interpulse delay of 15 s.

### 2.2. *In situ* heart preparation

Mature male Sprague-Dawley rats (420  $\pm$  20 g) fed *ad libitum* were used in the study. The open chest rat model described in detail by us previously was employed [20]. Briefly, the rats were initially anaesthetised with 50 mg.kg $^{-1}$  sodium pentobarbitone administered intraperitoneally. Following surgical preparation, animals were maintained under anaesthesia by infusion of 15 mg.kg $^{-1}$ .h $^{-1}$  sodium pentobarbitone via the femoral vein. Rats were intubated and artificially ventilated using a Harvard small animal ventilator.

Following instrumentation animals were placed in a temperature-controlled animal holder, a thoracotomy performed and a purpose built 6 mm diameter double-tuned surface coil with a flexible-arm was located on the left ventricular myocardium, as described by us previously [20]. The coil is positioned against the myocardium continuously throughout the cardiac cycle. Plastic film was then placed over the thorax to prevent heat loss and dehydration during the experiment. The animals were introduced into the horizontal bore of a 7 Tesla superconducting magnet, and animal temperature was continuously maintained at 37°C by a thermostatically regulated heating jacket. Magnetic field homogeneity throughout the sample volume was optimised on the  $^1\text{H}$  signal using a fifteen-channel Oxford Instruments shim supply.

$^{31}\text{P}$ -NMR spectra were acquired, without gating, at 121.46 MHz as described in detail previously [20].  $^{31}\text{P}$  acquisitions employed a 10-kHz sweep width and consisted of 10K data points. RF pulse-width was 53  $\mu\text{s}$  and the square pulses were optimised to yield a maximal signal intensity for a 90° sensitive volume extending to a maximum depth of 2.5 mm into the myocardium (see Ref. [20]). This procedure and small sample volume ensured minimal contamination from intra-ventricular blood with no contamination from adjacent tissues [20]. After a 30-min stabilisation period, a partially relaxed spectrum was acquired, consisting of 512 signal averaged free induction decays (FID's) acquired with an interpulse delay of 1.5 s. A fully relaxed  $^{31}\text{P}$  spectrum consisting of 512 signal

averaged FID's with a total interpulse delay of 21 s was then acquired, followed by a second partially relaxed spectrum. Initial and final spectra were acquired to assess metabolite stability during acquisition of the longer fully relaxed spectrum. FID's were multiplied by a Lorentzian line broadening factor of 25 Hz.

To quantitate spectral intensities an external reference of phenylphosphonic acid (PPA) was employed. The external reference consisted of a solution of 12.5 mM PPA and 120 mM KCl in deuterated water contained in a thin-walled latex balloon phantom located on the top of the NMR surface coil. The absolute concentration of PPA in the external reference was verified after experimentation by atomic absorption spectrophotometry. Total reference volume (~1.5 ml) substantially exceeded the sensitive volume of the coil. Thus  $B_1$  penetration and sample volumes are identical within tissue and reference, permitting straightforward calibration of spectral intensities. In preliminary characterisation experiments heart phantoms containing known standards were alternatively placed above and below the surface coil with the PPA reference on the opposite side. This verified the  $B_1$  symmetry along the vertical axis (less than a 5% difference between signal intensities and sample volumes above and below the coil), and the reliability of quantitation. The accuracy and ease of use of similar external reference calibration strategies has been examined recently [21].

### 2.3. Freeze-clamp analysis of tissue metabolites

In situ and isolated hearts were freeze-clamped in tongs cooled in liquid  $N_2$  [20]. Frozen wafers were stored at  $-80^\circ\text{C}$  until analysed. For analysis portions of the frozen tissue (~400 mg) were weighed, then pulverised under liquid  $N_2$ . The powder was added to 10 volumes of ice-cold 0.6 M perchloric acid and immediately homogenised. Following brief centrifugation (2 min at 10 000 rpm) supernatant was removed and neutralised by addition of 3 M KOH (to a pH of ~6.3). The neutralised sample was centrifuged and 100  $\mu\text{l}$  of supernatant analyzed for PCr, Cr, ATP, GTP, CTP and UTP using the HPLC method of Harmsen et al. [22]. Recovery of standards analysed in the same manner exceeded 94%. Total ATP content of heparinised freshly drawn whole blood was also assayed ( $n = 4$ ) using this HPLC method following acid extraction and neutralisation of samples.

### 2.4. Metabolic calculations

$^{31}\text{P}$ -Spectral intensities were determined by computer integration of natural line-shapes. Similar results were obtained by fitting spectral resonances to Lorentzian line-shapes prior to integration. To calculate ATP concentrations from NMR data ATP was assumed to equal 93% of the  $\beta$ -NTP (nucleoside triphosphate) intensity in isolated and in situ hearts based on the total tissue concentrations

of ATP GTP, CTP and UTP (see Section 3). This assumes equal visibility of ATP, GTP, CTP, and UTP in  $^{31}\text{P}$ -NMR spectra. From this point  $\beta$ -ATP refers to 93% of the  $\beta$ -NTP intensity. To check that potential noise or off-resonance elements in the  $\beta$ -NTP region did not significantly effect our data, we also calculated and compared the PCr/ $\gamma$ -NTP ratio in in situ hearts.

$^{31}\text{P}$ -NMR intensities for PCr and  $\beta$ -ATP in spectra from in situ hearts were calibrated using the equation:

$$[\text{Metabolite}] (\mu\text{mol.g}^{-1}) = (\text{MetaboliteIntensity} / \text{PPAIntensity}) \times 12.5 \mu\text{mol.g}^{-1}$$

Intensities for PCr and  $\beta$ -ATP in fully relaxed spectra from isolated perfused hearts were calibrated using the equation:

$$[\text{Metabolite}] (\mu\text{mol.g}^{-1}) = (\text{MetaboliteIntensity} / \text{MDPIntensity}) \times 35 \mu\text{mol.g}^{-1} \times (\text{BalloonVolume} / \text{HeartVolume})$$

Heart volume was determined from heart wet weight assuming an approximate density of  $1 \text{ g.ml}^{-1}$ . Balloon volume was measured from the calibrated syringe used to fill the ventricular balloon. NMR-determined and HPLC-determined metabolite contents are converted to  $\mu\text{mol.g}^{-1}$  dry wt. Total tissue water and tissue dry weights were determined by measuring tissue weights before and after overnight oven drying. Tissue water contents are shown in Table 1.

### 2.5. Calculation of free cytosolic [ADP], [5'-AMP] and [ATP]/[ADP].[ $P_i$ ]

To examine the impact of observed nucleotide levels on cellular metabolic state, we calculated free cytosolic [ADP], [5'-AMP] and the phosphorylation ratio ([ATP]/[ADP].[ $P_i$ ]) as described previously [20]. To calculate these indices tissue ATP, PCr and Cr concentrations were converted to mM based on the tissue water contents noted above, and the previously determined intracellular spaces of 40% and 73% of total tissue water for isolated and in situ hearts, respectively [20]. Free cytosolic [ADP] was calculated from the creatine kinase equilibrium:

$$[\text{ADP}] = [\text{ATP}].[Cr]/[PCr].K'_{ck}$$

Table 1  
Fluid compartments for in situ and Langendorff perfused rat hearts

	In situ hearts	Perfused hearts
% $\text{H}_2\text{O}$	$80 \pm 1\%$ wet wt	$85 \pm 2\%$ wet wt *
Total $\text{H}_2\text{O}$	$4.0 \pm 0.1 \text{ ml.g}^{-1}$ dry wt	$5.7 \pm 0.2 \text{ ml.g}^{-1}$ dry wt *
Extracellular	$1.1 \text{ ml.g}^{-1}$ dry wt	$3.4 \text{ ml.g}^{-1}$ dry wt
Intracellular	$2.9 \text{ ml.g}^{-1}$ dry wt	$2.3 \text{ ml.g}^{-1}$ dry wt

The % tissue  $\text{H}_2\text{O}$  is expressed relative to total wet weight. The remaining volumes (expressed per g dry weight) are based on % tissue  $\text{H}_2\text{O}$ , and previously measured intracellular volumes of 73% and 40% for in situ and Langendorff perfused rat hearts supplied with glucose a substrate, respectively [20]. \*  $P < 0.05$  vs. in situ hearts.

where  $[Cr]$  was determined from total creatine pool ( $[PCr] + [Cr]$ ) values of  $69.1 \pm 3.5$  and  $75.8 \pm 3.4 \mu\text{mol.g}^{-1}$  dry weight, determined by HPLC analysis of freeze-clamped isolated and in situ hearts, respectively, and  $K'_{ck}$  is the observed creatine kinase equilibrium adjusted for experimentally measured  $pH_i$  and  $[Mg^{2+}]_i$  according to the method of Lawson and Veech [23], but using the more recent dissociation constant provided in Teague and Dobson [24].  $[ATP]/[ADP].[P_i]$  was calculated from the free cytosolic  $[ADP]$  and tissue ATP and  $P_i$  concentrations. Since  $P_i$  was not consistently resolvable in in situ hearts, we use a previously determined value of 0.83 mM [20] in calculating basal  $[ATP]/[ADP].[P_i]$  in situ. Free cytosolic  $[5'-AMP]$  was determined from the adenylate kinase equilibrium:

$$[5' - AMP] = K'_{ak} \cdot [ADP]^2 / [ATP]$$

where  $K'_{ak}$  is the observed adenylate kinase equilibrium adjusted for experimentally measured  $pH_i$  and  $[Mg^{2+}]_i$ .

Since basal intracellular pH cannot be measured via  $^{31}\text{P}$ -NMR in situ due to poor resolution of the  $P_i$  resonance in the presence of blood 2,3-diphosphoglycerate, the pH of 7.3 determined previously for in situ rat hearts [20] was employed in calculating free intracellular  $Mg^{2+}$  concentrations and adjustment of enzyme equilibria for in situ hearts.

Free  $[ADP]$ ,  $[5'-AMP]$  and  $[ATP]/[ADP].[P_i]$  were calculated in four different ways: (i) solely from  $[ATP]$  and  $[PCr]$  values determined in the  $^{31}\text{P}$ -NMR experiments; (ii) from the HPLC determined total tissue  $[ATP]$  and the  $^{31}\text{P}$ -NMR-determined  $PCr/ATP$  ratio; (iii) from the HPLC determined total tissue  $[PCr]$  and the  $^{31}\text{P}$ -NMR-determined  $PCr/ATP$  ratio; and (iv) from the HPLC determined total tissue values for both  $[ATP]$  and  $[PCr]$ .

## 2.6. Statistics

Data is presented as mean  $\pm$  S.E.M. Statistical variations between values calculated using different methodologies were determined using a Student's *t*-test with Bonferroni's correction. A *P*-value of  $< 0.05$  was considered indicative of a statistically significant difference.

## 3. Results

### 3.1. Total tissue phosphates determined from HPLC analysis

HPLC analysis of freeze-clamped tissue yielded the nucleotide concentrations shown in Table 2. Note that there were only minor differences between nucleotide levels from in situ and isolated perfused hearts. ATP represents 93% and 94% of total triphosphates analyzed (ATP, GTP, CTP, UTP) in in situ and isolated perfused hearts, respectively. Total tissue PCr was significantly higher in in

situ compared with isolated hearts. Glucose and glucose + pyruvate perfused hearts displayed comparable total tissue ATP concentrations whereas total tissue PCr was significantly higher in glucose + pyruvate perfused hearts. In rat blood, total ATP content was calculated to be  $0.6 \pm 0.2 \mu\text{mol.ml}^{-1}$  ( $n = 4$ ).

### 3.2. $^{31}\text{P}$ -NMR-determined ATP and PCr concentrations

Typical fully relaxed  $^{31}\text{P}$ -spectra acquired from in situ and isolated perfused rat hearts are shown in Fig. 1. Basal  $PCr/\beta\text{-NTP}$  and  $PCr/\gamma\text{-NTP}$  ratios for in situ myocardium were calculated to be  $2.48 \pm 0.42$  and  $2.50 \pm 0.16$ , respectively, demonstrating minimal analytical differences in this preparation when using either  $\beta\text{-NTP}$  or  $\gamma\text{-NTP}$  resonances. Using the  $\beta\text{-NTP}$  resonance and correcting for contribution from other triphosphates  $^{31}\text{P}$ -NMR determined PCr concentrations are 1.5, 1.7 and 2.7-fold greater than ATP concentrations in glucose-perfused, glucose + pyruvate perfused, and in situ rat hearts, respectively (Table 2). In all models the  $^{31}\text{P}$ -NMR determined PCr values agreed well with HPLC determined total tissue concentrations. In isolated perfused hearts  $^{31}\text{P}$ -NMR and HPLC-determined ATP concentrations were also similar. However, in the heart in situ the  $^{31}\text{P}$ -NMR determined ATP concentration was only 71% of the HPLC-determined

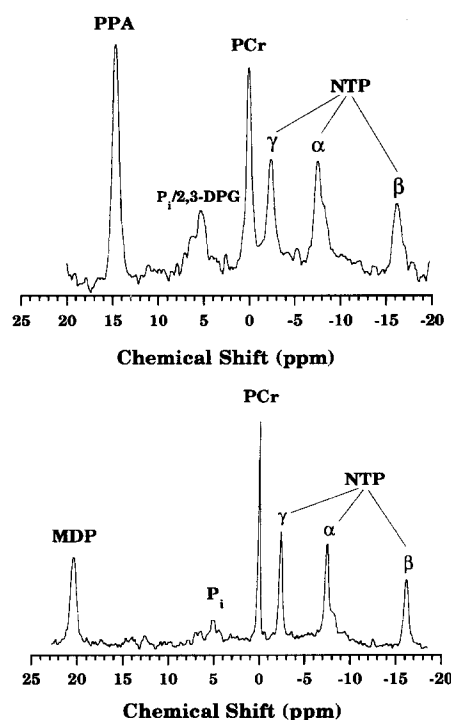


Fig. 1. Typical fully relaxed  $^{31}\text{P}$ -NMR spectra acquired from the in situ rat heart (upper panel) and from a Langendorff perfused rat heart supplied with glucose as substrate (lower panel). PPA, phenylphosphonic acid; MDP, methylene diphosphonate;  $P_i$ , inorganic phosphate; 2,3-DPG, 2,3-diphosphoglycerate; PCr, phosphocreatine; NTP, nucleoside triphosphate ( $\gamma$ ,  $\alpha$ , and  $\beta$ -resonances).

Table 2

Nucleotide and PCr concentrations determined by HPLC analysis of freeze-clamped tissues or from  $^{31}\text{P}$ -NMR data for in situ and isolated Langendorff perfused rat hearts

	HPLC-determined levels (total)			$^{31}\text{P}$ -NMR-determined levels (free)		
	Isolated (Gluc)	Isolated (Gluc + Pyr)	In situ	Isolated (Gluc)	Isolated (Gluc + Pyr)	In situ
ATP ( $\mu\text{mol.g}^{-1}$ )	21.0 $\pm$ 1.2	21.2 $\pm$ 1.0	26.3 $\pm$ 1.4 †	19.3 $\pm$ 0.9 (92%)	19.6 $\pm$ 1.0 (92%)	18.6 $\pm$ 3.2 * (71%)
PCr ( $\mu\text{mol.g}^{-1}$ )	29.4 $\pm$ 2.3	34.0 $\pm$ 2.1	49.8 $\pm$ 1.5 †	29.0 $\pm$ 1.8 (99%)	33.5 $\pm$ 3.0 (98%)	49.6 $\pm$ 8.4 † (99%)
PCr/ATP	1.4 $\pm$ 0.1 §	1.6 $\pm$ 0.1	1.9 $\pm$ 0.1 †	1.5 $\pm$ 0.1 §	1.7 $\pm$ 0.1	2.7 $\pm$ 0.2 † *
ADP ( $\mu\text{mol.g}^{-1}$ )	4.4 $\pm$ 0.1 §	3.6 $\pm$ 0.1	3.3 $\pm$ 0.2 †	0.20 $\pm$ 0.02 * § (5%)	0.16 $\pm$ 0.02 * (4%)	0.16 $\pm$ 0.05 * (5%)
AMP (nmol.g $^{-1}$ )	920 $\pm$ 105 §	645 $\pm$ 112	510 $\pm$ 80 †	2.16 $\pm$ 0.23 * § (0.2%)	1.27 $\pm$ 0.20 * (0.2%)	1.38 $\pm$ 0.48 † * (0.3%)
NTP ( $\mu\text{mol.g}^{-1}$ )	22.5 $\pm$ 1.5	23.4 $\pm$ 2.4	28.0 $\pm$ 1.5 †	–	–	–
$\frac{[\text{ATP}]}{[\text{ADP}][\text{P}_i]}$ ( $\text{mM}^{-1}$ )	–	–	–	29 $\pm$ 2 §	101 $\pm$ 14	148 $\pm$ 33 *

ATP and PCr were determined by HPLC analysis (total), or using  $^{31}\text{P}$ -NMR methods (free cytosolic). Isolated hearts were supplied with either glucose (Gluc) or glucose + pyruvate (Gluc + Pyr) as substrates.  $^{31}\text{P}$ -NMR-determined [ADP] and [AMP] are free concentrations calculated as outlined in Section 2. ADP, AMP and total NTP (ATP + GTP + CTP + UTP) were determined by HPLC. % visibilities based on HPLC-determined total tissue levels are given in parentheses. [ATP]/[ADP][ $\text{P}_i$ ] was calculated from free [ATP] and [ADP] values and NMR-determined [ $\text{P}_i$ ] as outlined in Section 2. All values are means  $\pm$  S.E.M. ( $n =$ ). \*  $P < 0.05$  vs. total tissue values; †  $P < 0.05$  vs. isolated heart values; §  $P < 0.05$  Gluc vs. Gluc + Pyr perfused hearts.

total tissue concentration. Consequently, while NMR and HPLC-determined PCr/ATP ratios were comparable for isolated perfused hearts (irrespective of substrate), the NMR determined PCr/ATP ratio for in situ myocardium was  $\sim 42\%$  higher than the value calculated from total tissue concentrations (Table 2).

Total tissue levels of ADP and 5'-AMP were much greater than the free cytosolic concentrations calculated from the creatine kinase and adenylate kinase equilibria (Table 2). Average  $K'_{\text{ck}}$  values used in calculation of free [ADP] in glucose perfused, glucose + pyruvate perfused and in situ hearts were  $119 \pm 7$ ,  $116 \pm 8$ , and  $61 \pm 3$ , respectively. Average  $K'_{\text{ak}}$  values used in calculation of free [5'-AMP] in glucose perfused, glucose + pyruvate perfused and in situ hearts were  $1.0 \pm 0.1$ ,  $1.0 \pm 0.1$ , and  $0.9 \pm 0.1$ , respectively. Based on total tissue and free cytosolic data, we have calculated that 5% of myocardial ADP and 0.2–0.3% of total 5'-AMP exists in a free form within the myocardium of the in situ and isolated perfused rat heart (Table 2).

### 3.3. Metabolic and bioenergetic parameters calculated using $^{31}\text{P}$ -NMR (free) and HPLC determined (total) ATP and PCr values

Owing to essentially complete NMR visibility of ATP and PCr in isolated perfused hearts independent of carbon substrate, there were no differences between metabolic and bioenergetic parameters calculated wholly from NMR data, or using total tissue [ATP] and/or [PCr] as internal references (Fig. 2). On the other hand, due to the difference in [ATP] measured using NMR versus HPLC in the heart in situ, significant differences emerged in derived metabolic and bioenergetic parameters for the in situ myocardium (Fig. 2). When calculated using the common approach of assigning total tissue [ATP] to the  $\beta$ -NTP intensity, free cytosolic [ADP] and [5'-AMP] values were substantially lower (by  $> 75\%$  and  $90\%$ , respectively) than values

calculated from the NMR-determined [ATP] and [PCr]. [ATP]/[ADP][ $\text{P}_i$ ] was therefore significantly higher (by  $> 600\%$ ) when calculated from total tissue [ATP] rather than the NMR-determined concentrations (Table 2). Owing to excellent agreement between NMR-determined and total tissue PCr values, use of total tissue [PCr] as an internal reference did not introduce any errors in calculation of [ADP], [5'-AMP], or [ATP]/[ADP][ $\text{P}_i$ ]. Use of both total tissue [ATP] and [PCr] leads to  $\sim 70\%$  overestimation of free [ADP] and [5'-AMP], whereas [ATP]/[ADP][ $\text{P}_i$ ] calculated using total tissue concentrations is in agreement with the wholly NMR-determined value (Fig. 2).

## 4. Discussion

$^{31}\text{P}$ -NMR-spectroscopy has been an important tool in advancing our knowledge of cardiovascular energetics and metabolism over the past decade, and continues to provide investigators with a means of non-invasively monitoring intracellular metabolism. One area of continuing controversy, relevant to both myocardial metabolism and the application of NMR spectroscopy, is subcellular compartmentation of nucleotides. As already noted, compartmentation represents both a challenge and a potential source of error for  $^{31}\text{P}$ -NMR spectroscopy. Although  $^{31}\text{P}$ -NMR spectroscopy is generally assumed to observe total myocardial ATP (and PCr) in perfused hearts, this has been questioned recently [9,10]. Unfortunately few studies adequately address the issue of NMR visibility since most fail to quantitate NMR intensities using an external reference (for example). Humphrey and Garlick [10] and Bak and Ingwall [11] have compared quantitation using HPLC and NMR, whereas other studies examine metabolite ratios or percent changes in metabolite levels during ischemia [12–15]. Moreover, no studies have compared NMR and HPLC quantitation of nucleotides in the in situ myocardium, despite the increased occurrence of in vivo studies in the

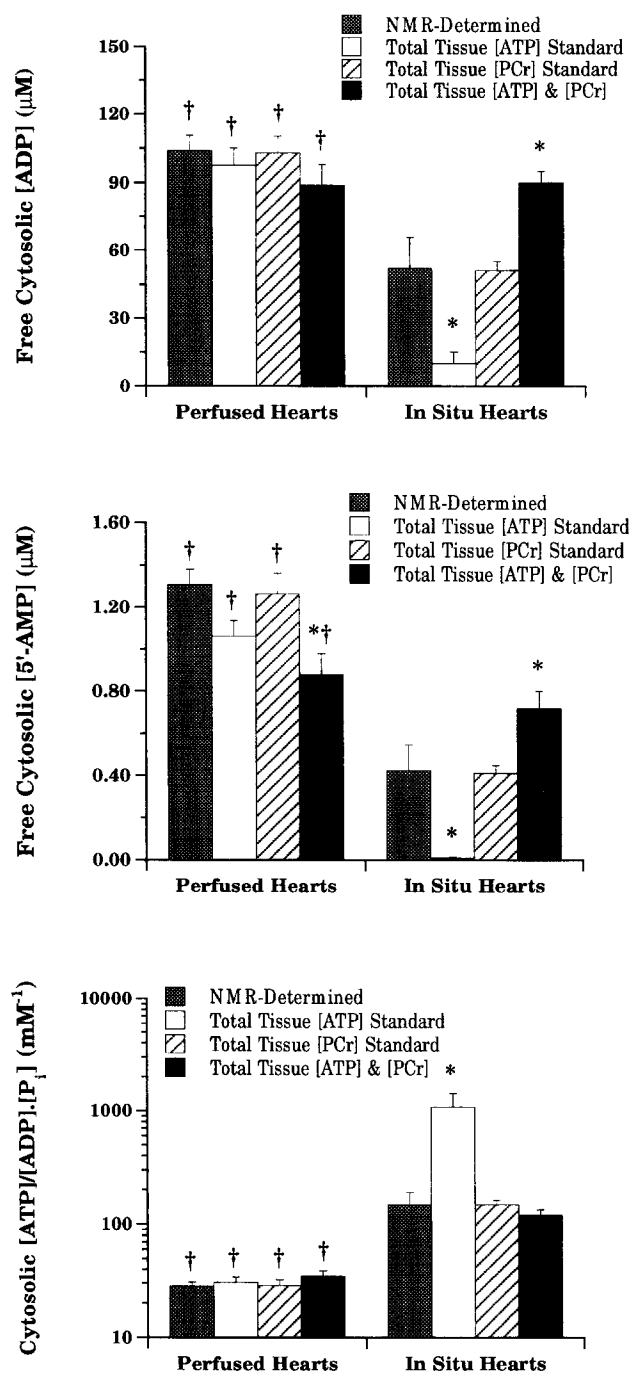


Fig. 2. Free cytosolic [ADP], [5'-AMP] and [ATP]/[ADP].[P<sub>i</sub>] for isolated Langendorff perfused hearts supplied with glucose as substrate, and in situ rat hearts. Values were calculated based on <sup>31</sup>P-NMR-determined PCr and ATP concentrations (NMR-Determined), HPLC-determined total tissue [ATP] and the NMR-determined PCr/ATP ratio (Total Tissue [ATP] Standard), HPLC-determined total tissue [PCr] and the NMR-determined PCr/ATP ratio (Total Tissue [PCr] Standard), and from HPLC-determined total tissue [ATP] and [PCr] (Total Tissue [ATP] and [PCr]). Values are means ± S.E.M. (n = 5). \* *P* < 0.05 vs. <sup>31</sup>P-NMR-determined values; † *P* < 0.05 vs. in situ heart values.

literature (e.g., Refs. [20,25,26]). The data presented here confirm recent observations of near 100% NMR visibility of ATP and PCr in perfused rat hearts [10,11]. In contrast,

in in situ myocardium the <sup>31</sup>P-NMR determined PCr/ATP ratio is considerably higher than the total tissue ratio. Assuming that <sup>31</sup>P-NMR cannot observe more ATP than is determined by HPLC analysis of frozen tissue, this PCr/ATP discrepancy in the in situ organ can only be due to: (1) up to 29% underestimation of total tissue [PCr] by HPLC analysis, and/or (2) less than 100% NMR visibility of ATP. We exclude the first possibility and support the second on the basis of: (1) excellent agreement between NMR and HPLC-determined [PCr] values in isolated and in situ hearts; and (2) an NMR-determined [ATP] which is 71% of the total tissue value in in situ hearts. It is concluded that ~29% of total tissue ATP is NMR invisible in the rat myocardium in situ.

#### 4.1. Compartmentation of myocardial ATP?

While our data support partial NMR-visibility of ATP in the myocardium in situ, the cellular location of this pool is unclear. Moreover, why ATP visibility in the in situ myocardium differs from that in the isolated perfused heart is also unknown, though several possibilities arise from our data. ATP does bind myofibrils [27], although it is generally agreed that this only accounts for 2–4% of total ATP. Some ATP may bind cellular ATPases and the extent of this binding remains to be determined. Mitochondrial ATP may be NMR invisible [9], possibly due to the proximity to paramagnetic ions [28]. This remains controversial [29]. Based on differences between total tissue [ATP] and NMR-determined [ATP], we estimate maximum possible mitochondrial ATP levels of 9% and 29% of total tissue ATP in isolated and in situ hearts, respectively. These values agree well with previous estimates of 7–30% [1–6,11,30]. Interestingly, previous estimates of mitochondrial ATP tend to be higher in more physiological working heart models, consistent with a potentially higher mitochondrial ATP in the myocardium in situ. In addition, since the in situ heart is more highly energised than the isolated heart, it is plausible that mitochondrial ATP is greater in situ. An energy-dependent decline in mitochondrial [ATP] upon isolation and perfusion of the heart is consistent with reductions in mitochondrial [ATP] during severe energy depletion (e.g., ischaemia) [31,32]. Moreover, recovery of depleted mitochondrial ATP is slow due to the absence of a mechanism to transport and accumulate cytosolic ATP into mitochondria. To examine the relationship between ATP visibility and energy state in perfused hearts, we supplied hearts with glucose + pyruvate as carbon substrates. As shown in Table 2 addition of pyruvate to the buffer markedly increased [ATP]/[ADP].[P<sub>i</sub>] ~3-fold. Nevertheless, PCr and ATP remained essentially fully NMR visible. Thus, there is no clear relation between energy state and NMR visibility. Interestingly, the magnitude of the NMR invisible pool in situ equals the total ATP lost upon isolation and perfusion of hearts (Table 2). Therefore, the NMR invisible ATP may well represent the

entire ATP pool lost during the transition from in situ to isolated perfused heart.

In addition to the energetic difference between perfused and in situ hearts, fluid compartmentation differs substantially (Table 1). Upon isolation and perfusion of the rat heart, total tissue water increases by  $\sim 40\%$ , primarily reflecting extracellular oedema (i.e., an extracellular volume increase of  $\sim 300\%$ ), together with a minor redistribution of water from the intra- to extracellular space (i.e., a  $\sim 20\%$  decline in intracellular volume). These fluid changes are consistent with observations of Polimeni and Buraczewski [33]. While they may play some role in modifying cellular energetics and function, these fluid changes are unlikely to be involved in the loss of NMR-invisible ATP. Since cytosolic volume is reduced by  $\sim 20\%$ , cytosolic solute concentrations are actually elevated. It seems unlikely that an increase in concentration would stimulate release of bound/NMR invisible ATP from intracellular sites.

Another possibility deserving a mention is a contribution to  $^{31}\text{P}$ -spectra from an acid-insoluble nucleotide or nucleotide complex. Mowbray and colleagues recently discovered and characterised a polymeric nucleotide complex in rat heart [34]. This is thought to represent from 25% to 55% of the total nucleotide content of the heart. It is possible that such a molecule may contribute to the  $\gamma$ ,  $\alpha$ , and  $\beta$ -P resonances in  $^{31}\text{P}$ -spectra resulting in an apparent discrepancy between chemically determined and NMR estimated ATP levels. However, the molecule's large size, localisation to mitochondrial membranes, and binding to specific phosphodiesterases [35] will limit its NMR visibility in the heart. Moreover, despite the compound being present in high quantities in the perfused heart [34], the excellent agreement between total tissue and NMR-determined ATP for isolated hearts observed here and by others [10,11] argues against this possibility. It therefore seems unlikely that discrepancies between total tissue and NMR-determined ATP result from detection of this type of metabolite in vivo. On the other hand, it has been suggested that myocardial ATP itself is not completely acid extractable, with  $\sim 13\%$  remaining undetected [36]. If this is so, the difference between perchloric acid-extracted total tissue ATP and  $^{31}\text{P}$ -NMR visible ATP may in fact exceed that observed here for isolated and in situ rat hearts.

Finally, we exclude a significant error in analysis of in situ data due to a greater contribution of blood ATP in freeze-clamped tissue extracts versus in situ spectra. Blood contamination of frozen hearts can only explain less than a 4% difference between  $^{31}\text{P}$ -NMR-determined and total tissue ATP contents (i.e.,  $< 1 \mu\text{mol ATP.g}^{-1}$  dry weight). This is based on a maximal estimated blood content of  $\sim 0.3 \text{ ml.g}^{-1}$  wet weight (i.e., vascular and ventricular volumes of 10% and 20%, respectively), and a measured blood ATP content of  $0.6 \mu\text{mol.ml}^{-1}$  (see Results). Moreover, the presence of 2,3-DPG in  $^{31}\text{P}$ -spectra indicates that  $^{31}\text{P}$ -NMR analysis does detect some of the blood signal.

The functional significance of distinct ATP pools in the in situ myocardium is unclear. However, a number of studies support functional compartmentation of myocardial ATP. For example, sarcolemmal and sarcoplasmic reticulum coupled glycolytic enzymes are capable of ATP production, and this ATP is preferentially utilised for maintenance of ion homeostasis [37,38]. Glycolytic ATP may also preferentially support ischaemic myocardium (for review, see [39]). Indeed, inconsistent relationships between total ATP and function during ischaemia led to the suggestion of compartmentalised ATP in cardiac muscle. Whether NMR invisible ATP reflects functional pools such as these remains to be determined. Future studies might address relative changes in visible and invisible ATP during ischaemia, as has been done in the isolated perfused heart [9,10].

#### 4.2. Compartmentation of ADP and 5'-AMP

In contrast to ATP, myocardial ADP and 5'-AMP are almost completely NMR invisible in isolated perfused and in situ myocardium. The currently measured ADP and 5'-AMP compartmentation agrees well with data of Bunger and Soboll for perfused guinea pig hearts [1]. Cellular ADP is considered largely bound to actomyosin in the intact myocardium, and data support significant compartmentation of 5'-AMP within the mitochondria [1,2]. The observation that less than 1% of total 5'-AMP exists freely in the cytosol is consistent with very low levels of 5'-AMP catabolites produced in normoxic myocardium despite the presence of highly active catabolic enzymes [1,18]. Indeed,  $\sim 100 \text{ nmol.min}^{-1}.\text{g}^{-1}$  of 5'-AMP preferring 5'-nucleotidase activity exists in the cytosol of rat myocytes [40], and the enzyme possesses a  $K_m$  up to 2-orders of magnitude greater than the free 5'-AMP concentration. With respect to dephosphorylation of cytosolic 5'-AMP, the physiologically active catabolite adenosine is highly potent and only low levels are required to produce its reportedly important physiological actions [18,41]. Consequently, only minimal levels of 5'-AMP need be exposed to cytosolic 5'-nucleotidase [1,18]. 5'-AMP compartmentation may therefore balance formation of the regulatory compound adenosine with conservation of the myocardial nucleotide pool.

#### 4.3. Impact of compartmentation on determination of bioenergetic indices: NMR calibration strategies

Apart from the identity and physiological significance of the NMR invisible ATP compartment, it is important to determine the impact of this observation on current analytical approaches to the estimation of myocardial metabolic and bioenergetic state. Presently, the most common calibration strategy in in vivo NMR studies involves use of total tissue [ATP] as an internal reference. Total tissue [ATP] is equated with NMR observed  $\beta$ -NTP, and [PCr]

and  $[P_i]$  are then determined from the  $^{31}\text{P}$ -NMR  $[\text{PCr}]/[\text{ATP}]$  and  $[\text{ATP}]/[P_i]$  ratios. Alternatively, total tissue  $[\text{PCr}]$  may also be equated with the NMR-observed  $\text{PCr}$ . If myocardial ATP is not 100% NMR visible then these calibration strategies are all erroneous.

Since  $^{31}\text{P}$ -NMR does observe essentially all ATP and  $\text{PCr}$  in Langendorff perfused hearts (Table 2), there are no substantial errors in estimation of metabolic parameters for the isolated heart, irrespective of the analytical approach taken (Fig. 2). However, in the in situ heart use of total tissue  $[\text{ATP}]$  and the NMR-determined  $\text{PCr}/\text{ATP}$  ratio results in  $>75\%$  underestimation of free cytosolic  $[\text{ADP}]$ . Consequently, free  $[5'\text{-AMP}]$  is underestimated by more than 90%, and  $[\text{ATP}]/[\text{ADP}][P_i]$  overestimated by more than 600% (Fig. 2). Use of both total tissue  $[\text{ATP}]$  and  $[\text{PCr}]$  values results in significant overestimation of free  $[\text{ADP}]$  and  $[5'\text{-AMP}]$ , but results in a comparable estimate of  $[\text{ATP}]/[\text{ADP}][P_i]$  (Fig. 2). In short, the data in Fig. 2 show that the method yielding the greatest differences is currently one of the most commonly employed calibration strategies in in vivo and in vitro NMR studies (e.g., see [18,20,25,26,42]). The data indicate that without direct quantitation of  $^{31}\text{P}$  spectral intensities, total tissue  $[\text{PCr}]$  may in fact represent a better metabolite for calibration of in situ spectra than tissue  $[\text{ATP}]$ .

## 5. Conclusions

In summary, the present results demonstrate a significant NMR invisible ATP pool in the in situ myocardium, approximating 29% of total tissue ATP. On the other hand, our data confirm 100% NMR visibility of ATP in the isolated perfused heart. The physiological relevance and intracellular location of the invisible ATP pool in in situ myocardium remains to be identified. Nevertheless, the discrepancy between total tissue and NMR visible ATP introduces significant errors in metabolic indices derived from NMR data using current methodologies. We suggest that total tissue  $[\text{PCr}]$  may actually represent a better metabolite than  $[\text{ATP}]$  in calibrating in situ spectral data.

## Acknowledgements

We are grateful for the helpful discussions with Dr. G.P. Dobson. This research was supported in part by grants from the National Heart Foundation of Australia (G 93B 3769) and the Australian Research Council.

## References

- [1] Bunger, R. and Soboll, S. (1986) *Eur. J. Biochem.* 159, 203–213.
- [2] Geisbuhler, T., Altschuld, R.A., Trewyn, R.W., Ansel, A.Z., Lamka, K.B. and Brierley, G.P. (1984) *Circ. Res.* 54, 536–546.

- [3] Kauppinen, R.A., Hiltunen, J.K. and Hassinen, I.E. (1980) *FEBS Lett.* 112, 273–276.
- [4] Hohl, C., Ansel, A., Altschuld, R.A. and Brierley, G.P. (1982) *Am. J. Physiol.* 242, H1022–H1030.
- [5] Arrio-Dupont, M. and De Nay, D. (1986) *Biochim. Biophys. Acta* 851, 249–256.
- [6] Humphrey, S.M., Buckman, J.E. and Hollis, D.G. (1990) *Eur. J. Biochem.* 191, 755–759.
- [7] Ingwall, J.S. (1982) *Am. J. Physiol.* 242, H729–H744.
- [8] Gadian, D.G. and Radda, G.K. (1981) *Ann. Rev. Biochem.* 50, 69–83.
- [9] Takami, H., Furuya, E., Tagawa, K., Seo, Y., Murakami, M., Watari, H., Matsuda, H., Hirose, H. and Kawashima, Y. (1988) *J. Biochem. (Tokyo)* 104, 35–39.
- [10] Humphrey, S.M. and Garlick, P.B. (1991) *Am. J. Physiol.* 260, H6–H12.
- [11] Bak, M.I. and Ingwall, J.S. (1992) *Am. J. Physiol.* 262, E943–E947.
- [12] Armiger, L.C., Headrick, J.P., Jordan, L.R. and Willis, R.J. (1996) *J. Mol. Cell. Cardiol.*, in press.
- [13] Lavanchy, L., Martin, J. and Rossi, A. (1985) *J. Physiol. (Paris)* 80, 196–201.
- [14] Jeffrey, F.M., Storey, C.J., Nunnally, R.L. and Malloy, C.R. (1989) *Biochemistry* 28, 5323–5326.
- [15] Herijgers, P., Overloop, K., Toshima, Y., Van Hecke, Vanstapel, F., Mubagwa, K. and Flameng, W. (1994) 89, 50–60.
- [16] Murphy, E., Gabel, S.A., Funk, A. and London, R.E. (1988) *Biochemistry* 27, 526–528.
- [17] Desmoulin, F., Cozzone, P.J. and Canioni, P. (1987) *Eur. J. Biochem.* 162, 151–157.
- [18] Headrick, J. and Willis, R.J. (1990) *Am. J. Physiol.* 258, H617–H624.
- [19] Headrick, J.P. and Willis, R.J. (1991) *J. Mol. Cell. Cardiol.* 23, 991–999.
- [20] Headrick, J.P., Dobson, G.P., Williams, J.P., McKirdy, J.C., Jordan, L.R. and Willis, R.J. (1994) *Am. J. Physiol.* 267, H1074–H1084.
- [21] Buchli, R., Martin, E. and Boesiger, P. (1994) *NMR Biomed.* 7, 225–230.
- [22] Harmsen, E., De Tombe, P.P. and De Jong, J.W. (1982) *J. Chromatogr.* 230, 131–136.
- [23] Lawson, J.W.R. and Veech, R.L. (1979) *J. Biol. Chem.* 254, 6528–6537.
- [24] Teague, W.E. and Dobson, G.P. (1992) *J. Biol. Chem.* 267, 14084–14093.
- [25] Katz, L.A., Swain, J.A., Portman, M.A. and Balaban, R.S. (1989) *Am. J. Physiol.* 256, H265–H274.
- [26] Robitaille, P.M., Merkle, H., Lew, B., Path, G., Hendrich, K., Lindstrom, P., From, A.H., Garwood, M., Bache, R.J. and Ugurbil, K. (1990) *Magn. Reson. Med.* 16, 91–116.
- [27] McClellan, G., Weisberg, A. and Winegrad, S. (1983) *Am. J. Physiol.* 245, C423–C427.
- [28] Bailey, I.A., Williams, S.R., Radda, G.K. and Gadian, D.G. (1981) *Biochem. J.* 196, 171–178.
- [29] Garlick, P.B., Brown, T.R., Sullivan, R.H. and Ugurbil, K. (1983) *J. Mol. Cell. Cardiol.* 15, 855–858.
- [30] Soboll, S. and Bunger, R. (1981) *Hoppe-Seyler's Z. Physiol. Chem.* 362, 125–132.
- [31] Asimikis, G.K. and Conti, V.R. (1984) *J. Mol. Cell. Cardiol.* 16, 439–448.
- [32] Asimakis, G.K., Sandhu, G.S., Conti, V.R., Sordahl, L.A. and Zwischenberger, J.B. (1990) *Circ. Res.* 66, 302–310.
- [33] Polimeni, P.I. and Buraczewski, S.I. (1988) *J. Mol. Cell. Cardiol.* 20, 15–22.
- [34] Patel, B., Sarcina, M. and Mowbray, J. (1994) *Eur. J. Biochem.* 220, 663–669.
- [35] Mowbray, J. and Patel, B. (1993) *Adv. Enzyme Regul.* 33, 221–234.
- [36] Bessho, M., Ohsuzu, F., Yanagida, S., Sakata, N., Aosaki, N., Tajima, T. and Nakamura, H. (1991) *Anal. Biochem.* 192, 117–124.



- [37] Hardin, C.D., Raeymaekers, L. and Paul, R.J. (1992) *J. Gen. Physiol.* 99, 21–40.
- [38] Xu, K.Y., Zweier, J.L. and Becker, L.C. (1995) *Circ. Res.* 77, 88–97.
- [39] Opie, L.H. (1989) in *Pathophysiology of Severe Ischemic Myocardial Injury* (Piper, H.M., ed.), pp. 41–65. Kluwer Academic Publishers, Dordrecht, The Netherlands.
- [40] Kochan, Z., Smolenski, R.T., Yacoub, M.H. and Seymour, A.-M.L. (1994) *J. Mol. Cell. Cardiol.* 26, 1497–1503.
- [41] Olsson, R.A. and Pearson, J.D. (1990) *Physiol. Rev.* 70, 761–845.
- [42] From, A.H.L., Zimmer, S.D., Michurski, S.P., Mohanakrishnan, P., Ulstad, V.K., Thoma, W.J. and Ugurbil, K. (1990) *Biochemistry* 29, 3731–3743.